Applications of Quantum Dots in the Biological Sciences

Shubeur Rahman
Department of Scientific Computing
Simula Research Laboratory,
Martin Linges v 17, Fornebu P.O.Box 134, 1325 Lysaker, Norway

January 15, 2008

Preface

This work identifies possible applications of nanoclusters or "quantum dots" in biological sciences. Of particular interest is the computational modelling of the nanoclusters. The quantum mechanical nature of these systems coupled with the complexity arising from their multi-particle nature, mean that ab-intio quantum many-body methods are necessary. A brief overview of ab-initio methods is also provided.

Contents

List of Abbreviations

Abbreviation	Description
CdS	Cadmium Sulphide
CdSe	Cadmium Selenide
DFT	Density Functional Theory
FRET	Fluorescence Resonance Energy Transfer
MD	Molecular Dynamics
PDE	Partial Differential Equation
QDs	Quantum Dots
QMC	Quantum Monte Carlo
TDDFT	Time Dependent Density Functional Theory
TEM	Transmission Electron Micrograph

Chapter 1

Quantum Dots in Biology

In recent years, significant experimental progress has been made in the use of nanoscale particles for biological applications. The particles are referred to as "nanoparticles", "nanocrystal" "nanoclusters", or "quantum dots" depending on the context. The experimental achievements include drug and gene delivery [1, 2], bio-detection of pathogens [3], detection of proteins [4], probing DNA structure [5], tissue engineering [6, 7] and in fluorescence microscopy [8, 9, 10]. In particular, the application of quantum dots as fluorescent probes holds promise for significant advances in medical imaging and biological research.

The achievements have laid the foundations for theorectical investigations to enable advances in the understanding of the fundamental structure, stability, and aqueous assembly of nanoparticle architectures. The physical systems consist of between 10s and 1000s of atoms, the complexity of which requires numerical methods for a reliable description. In particular, in order to address the quantum mechanical nature of these systems, numerical techniques known as "ab-initio" methods are necessary. These are discussed in Chapter 2.

This chapter begins with an overview of some of the relevant physics underlying the use of quantum dots in biomedical applications, and is followed by a summary of some of the key applications themselves. To conclude the chapter, an overview of the key results already achieved in the ab-initio modeling of nanocrystals for biomedical applications is given.

1.1 Semiconductor Quantum Dots and Nanocrystals

Quantum dots are semiconductor nanostructures where the charge carriers such as conduction band electrons and valence band holes are confined in three spatial dimensions. The confinement may be the result of the electrostatic potential of external gates as in GaAs/AlGaAs heterostructures for example or the presence of a semiconductor surface as in colloidal quantum dots. The confinement results in discrete energy levels which the charge carriers may occupy.

Quantum dots defined by lithographically patterned gate electrodes, or by etching on two-dimensional electron gases in semiconductor heterostructures can have lateral dimensions exceeding 100 nm.

Colloidal semiconductor quantum dots are "isolated" and free-standing quantum dots which can be as small as 2-10 nm, corresponding to 10-50 atoms in diameter and a total of 100-100000 atoms within the quantum dot volume. They are crystalline solids typically produced in solution. The nanocrystals are predominantly II-VI materials such as CdSe, CdTe, CdS, HgSe, HgTe, PbSe, ZnS etc. They have a direct bandgap with energies corresponding to the visible spectrum and chemical properties suitable for the preparation of colloidal dispersions and organically capped clusters. The most common ones are CdS, CdSe.

A key feature of the colloidal quantum dots is the strong dependence of the optical and physical properties on their size. The strong size-dependence is mainly a result of two factors. Firstly, as the size of the nanocluster is reduced, the proportion of the surface atoms to interior atoms increases and, as a result, surface effects such as relaxation, rearrangement of dangling bonds and defects become important. Secondly, as the cluster size is reduced, the density of states decreases and the excitons (electron-hole pairs) become increasingly confined. As a result, the size of the nanocrystals determine the linear and non-linear optical properties, luminescence wavelengths, and electrical properties. For example, for CdS, as the crystal size is varied from the molecular to the macroscopic regime, the band gap varies from 4.5 and 2.5 eV [11], and the melting point increases from 400° C to 1600° C [12].

1.2 Optical Properties

1.2.1 Band Gaps

The optical properties of colloidal quantum dots have been utilised in fluorescence microscopy. The frequencies of light absorbed and those emitted are affected by the band gap of the material. The band gap, denoted by E_{gap}, is an important physical characteristic of a pure, defect-free semiconductor. Above this energy gap is a band of energy states known as the conduction band, and below the energy gap is a band of energy states known as the valence band as shown in Figure 1.1. The lowest energy in the conduction band of an idealised one-dimensional semiconductor is usually denoted by E_c and the highest energy in the valence band by E_v. Then E_{gap} is the energy difference E_c-E_v. The electrical and optical energies of the band gap are related through $E_{gap} = \frac{hc}{\lambda}$, where h is Plancks constant, and c and λ are the speed and wavelength of light, respectively. The quantum dots will absorb light only of wavelengths shorter than that determined by the band gap value. For example, bulk CdS has a band gap of 2.42 eV, which corresponds to a wavelength of 512 nm [13]. The CdS nanoparticles begin to absorb light at 512 nm with absorbance continues into the UV (i.e. shorter wavelengths). As particle size declines, the band gap increases, and the absorbance onset shifts to shorter wavelengths as illustrated in Figure 1.4.

1.2.2 Fluorescence

The band gap also determines particle fluorescence. Fluorescence occurs when the absorption of a photon triggers an emmission of another photon with lower energy or longer wavelength. The energy difference between the absorbed and emmited photone is lost to atomic vibrations. Usually the absorbed photon is in the ultraviolet range, and the emitted light is in the visible range, but this depends on the absorbance curve and Stokes shift of the particular fluorophore. As the band gap decreases, a smaller amount of energy is dissipated through fluorescent emission to return to the ground state, and the wavelength of emitted light will shift to the red (Figure 1.4). As the band gap is inversely proportional to quantum dot size, larger quantum dots display red-shifted emission.

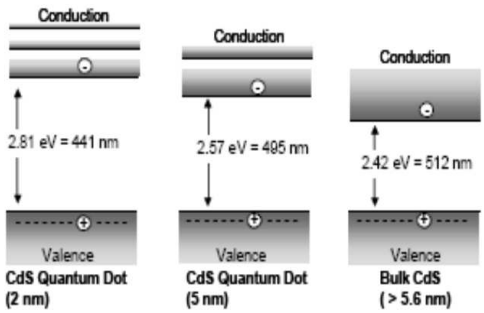

Figure 1.1: The band gap E_{gap} increases with decreasing quantum dot size and is inversely related to absorbance onset (λ_l) through the relationship $E = \frac{hc}{\lambda_l}$. Therefore, smaller particles begin to absorb at shorter wavelengths [14]. Figure taken from [15].

1.3 Quantum Dots for Biological Applications

The main challenges in the application of quantum dots to biological experiments are the necessity for the systems to operate in an aqueous environment, and for the nanoparticles to bind with high specifity to target biomolecules.

The quantum dots are often prepared at high temperatures and in non-polar organic solvents and are not necesarily water soluble. Water solubility can be achieved by functionalizing the quantum dots by certain organic compounds such as mercaptoacetic acid [9] or coated with a hydrophilic layer such as silica [8]. A number of quantum dot solubilisation strategies have been developed during recent years, including ligands such as peptides [17], dendrons [18] and polymer beads [19].

Biomolecular binding specifity may be achieved through conjugating quantum dots with ligands that bind selectively to specific subcellular structures. For example, ligands containing either an amine or carboxyl group, for instance, may enable cross linking molecules containing a thiol group [20, 21] or an N-hyroxysuccinimyl ester moiety. A nanoparticle may also be functionalised to bind with several biomolecules producing multi-potent probes.

The quantum dots are often passivated with a thin layer of a different inorganic crystal. For example, the surface of CdSe quantum dots are passi-

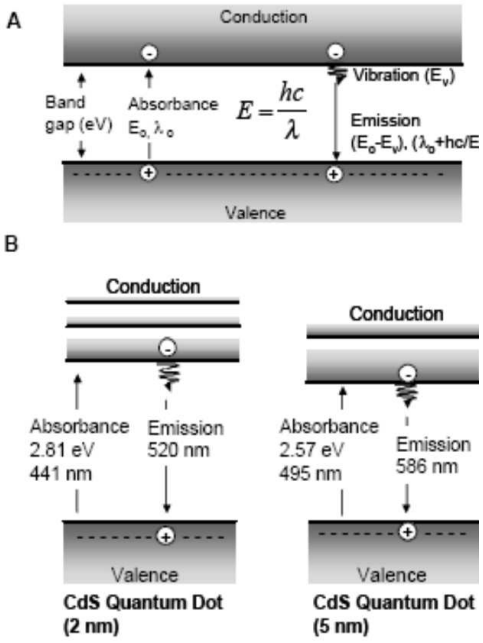

Figure 1.2: Fluorescent Emission and Particle Band Gap. (A) Photon absorption creates an excited electron. This electron loses some energy to heat; then decays to ground, emitting a photon. The emitted photon has a longer wavelength than the absorbed photon because of the energy lost to heat. (B) As the band gap decreases, the particle will absorb at longer wavelengths. This will produce a concomitant red-shift in particle fluorescent emission. Figure taken from [15].

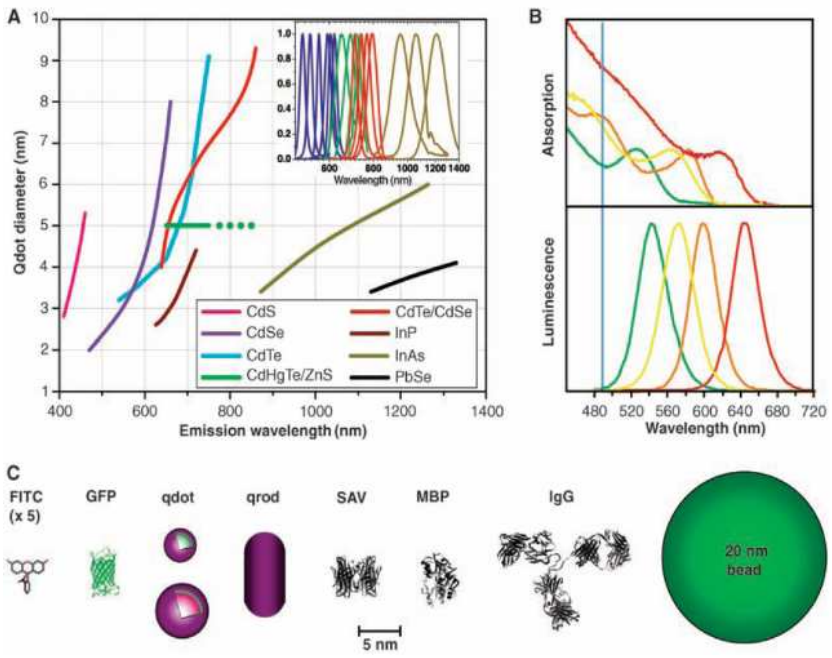

Figure 1.3: (A) Emission maxima and sizes of quantum dots of different composition. The curves represent experimental data from the literature on the dependence of peak emission wavelength on quantum dot diameter. The range of emission wavelength is 400 to 1350 nm, with size varying from 2 to 9.5 nm (organic passivation/solubilization layer not included). All spectra are typically around 30 to 50 nm (full width at half maximum). Inset: Representative emission spectra for some materials. (B) Absorption (upper curves) and emission (lower curves) spectra of four CdSe/ZnS qdot samples. The blue vertical line indicates the 488 nm line of an argon-ion laser, which can be used to efficiently excite all four types of qdots simultaneously. (C) Size comparison of qdots and comparable objects. FITC, fluorescein isothiocyanate; GFP, green fluorescent protein; qdot, green (4 nm, top) and red (6.5 nm, bottom) CdSe/ZnS qdot; qrod, rod-shaped qdot. Three proteinsstreptavidin (SAV), maltose binding protein (MBP), and immunoglobulin G (IgG)have been used for further functionalization of qdots. Figure and caption taken from Michalet *et al.* [16].

vated by a ZnS layer surface, protecting it from oxidation, preventing leeching of the Cd or Se into the aqueous environment and also produces a substantial improvement in the photoluminescence yield.

1.4 Biological Applications

Quantum dots have been explored in a number of biological settings with the objective of enhancing biomedical technology. Interest in the use of quantum dots in biomedicine began in 1998 after pioneering work by Alivisatos, *et al.* [8] and Chan *et al.* [9], who employed CdSe/ZnS quantum dots as fluorescent labels. Coupling the quantum dots directly to biorecognition molecules (e.g., antibodies, proteins), the particles could be targeted to particular parts of the cell, producing a fluorescent indicator.

Traditionally, organic fluorescent dyes are used for biological labeling. However, quantum dots have several advantages in comparison to organic dyes including the following:

A higher quantum yield. The quantum yield or brightness of organic dyes is reduced by molecular interactions with themselves, and the solvent. The passivation of a quantum dot with a protective inorganic layer lessons its susceptibility to these interactions and allows greater quantum yields [22].

Reduced photobleaching. This is the loss of fluorescence that occurs when dye molecules are exposed to light, resulting in the end in a non-fluorescent product. This is negligible in quantum dots and, as a result of reduced photobleaching, quantum dots can exhibit continuous fluorescence for a time period an order of magnitude greater than organic fluorescent dyes [9].

Size tunable excitation spectra. The spectra of ordinary dyes depend only on the material and thus is not variable. Quantum dots possess a wide absorbance-bandwidth (> 40 nm) while at the same time a narrow emission bandwidth ($\sim$ 20-30 nm). Thus a range of quantum dots can be excited by a single wavelength of light, and each of the excited quantum dots emits at a selected wavelength. This allows multi-plexed imaging.

These advantageous characteristics of quantum dots are utilised in a range biological applications. The use of quantum dots has often extended the scope of experiments to novel and exciting research areas.

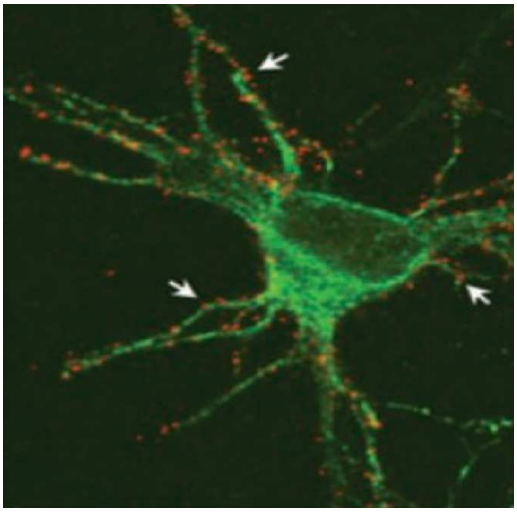

Figure 1.4: Red fluorescence from quantum dots due to presence of glycine receptors in a neuron. Figure taken from [23].

1.4.1 Fluorescent Labelling of Cells

The use of quantum dots for fluorescent labeling of cells has led not only to enhancements over fluorescent dyes, but has also extended the potential applications of fluorescent labels in biological systems. The new applications include those discussed below.

Cellular labels is in the study of cell motion. The motility and migration of cancerous cells are extremely detrimental properties that lead to metastases and formation of secondary tumors. Cell migration can be studied through the detection of phagokinetic tracks left behind by migrating cells [24]. A small size would be a basic prerequisite for the ideal systems to be used to monitor such tracks. Previuosly, relatively large sized Au particles (> 0.1 microns) were used to monitor the tracks but they perturbed cell mobility and also did not adhere well to the substrate. Quantum dots on the other hand, with their smaller sizes and low susceptibilty to bleaching are better suited for such investigations. In fact, quantum dots were able to distinguish between cancerous and noncancerous cells and remained luminescent for over one week [24].

Identification of specific cell types. Cell distinction is conventionally per-

formed by observation of phenotype or by fluorescently tagging uniquely expressed bio-markers. However, phenotype distinction requires detailed inspection of individual cells and is difficult to automate, limiting its use in high throughput applications. The fixed emission spectra of fluorescent molecules obscure the labeling of multiple desired cell types in a mixed population. The size-tunable and narrow emmisison spectra of quantum dots prove critically advantageous for such aaplications. Reserachers have performed multi-plexed imaging of cells for up to 5 distinct cell types and promise of even greater number [25]. More recently, quantum dots conjugated with tumor targeting ligands have been used to identify human prostate cancer cells in mice in *in vivo* conditions [26].

Detection of single molecules. The tracking of single molecules within a biological environment has been conventionally performed throught the use of fluorescent beads such as rhodaminne. The large size of the molecules (upto a micron) in comparison to biological environments has restricted the applicabilty of such systems. However, quantum dots which can be as small as a nanometer, may well be employed to track the motion of biomolecules in confined locations. In recent work, reserachers tracked individual glycine receptors and analysed their dynamics in the neuronal membrane of living cells for periods ranging from milliseconds to minutes [23]. Thus, quantum dots have been shown to provide real-time monitoring of biomolecules in living cells.

1.4.2 *In Vivo* Applications

The use of quantum dots for in-vivo applications could yield novel methods for disease identification and treatment. However, in-vivo applications must overcome obstacles associated with light propagation in tissue. The penetration of excitation and emission light can be difficult *in vivo*, as tissue is transparent to light only in a limited spectral range, mostly at longer, infrared wavelengths [27, 28].

Also of concern is the toxity of cadmium particles [29] which are frequently a constituent of nanoparticles. Surface passivation can significantly reduce the risk of exposure to free cadmium [30], and although the long-term effects of nanoparticle exposure have not yet been investigated; short-term *in vivo* studies do not demonstrate any acute effects.

In vivo applications of quantum dots are discussed in the following paragraphs.

Monitoring embryogenesis. Researchers have tracked the movement of structures in an embryonic frog as it matured to a tadpole, through the use of quantum dots [20]. Aqueous solutions of the quantum dots (approx 10^9 particles) were injected into a single cell of the frog embryo and were sucessfully transferred from parent to daughter cells during cell division. The quantum dots remained fluoresecnt for several cell division cycles and showed no sign of toxicity which would not be possible with conventional fluorescent dyes. Such techniques may faciliate a better understanding of cell development and lead to the prevention of birth defects.

Imaging structures within the body. Currently, vasculature is visualized using fluorescent dextrans. Some of the most challenging regions to image with these molecules are skin and adipose (i.e., fat) tissue because of their high degree of light scattering. Using quantum dots in living mice, researchers were able to visualize capillaries several hundred micrometers below the surface of the skin [31]. Producing the same image with dextran dyes required five times as much power and was much less detailed. With their narrow bandwidths and high quantum yields, nanoparticles provide improved imaging capabilities to dextran dyes.

Tracking the in vivo motion of biomolecules and cellular structures over time [32]. Fluorescent dyes, with their high susceptibility to photo-bleaching, are difficult to use in this context. However, nanoparticles can be used to monitor the motion of proteins, peptides, antibodies, or therapeutic agents in real time. [31] For example, when quantum dots were conjugated to peptides that bound the lung and tumor vasculature, they could be visualized in vivo [33]. Eventually, these techniques could be used to improve drug delivery and understand biomolecule circulation in the body.

Therapeutic contexts. Quantum dots can be used to image and even penetrate cancer cells, through receptor-mediated endocytosis [34]. Particles can be coupled to therapeutic agents, which are activated in the presence of light excitation. Gold nanoshells conjugated to recognition molecules can be used to image tumors. When they are optically excited they produce heat. Depending on the size of the nanoshell, heat production can be significant enough to kill the attached cells. Additional systems are envisioned that could release therapeutic agents, including chemotherapy drugs, upon light activation [35]. By only targeting the cells of interest, systems for localized drug delivery could significantly reduce the toxic effects of chemotherapy. These ideas take advantage of the combined electrical and optical properties of quantum dots, and serve as models toward the development of other

combined optoelectronic systems, including neuroelectronic interfaces.

1.4.3 Quantum Dot Biosensors

In the area of biosensors, QDs are particularly attractive due to their long-term photostability, allowing real-time and continuous monitoring.

Biosensors detect molecules of biological significance through an optical or electrical signal produced upon analyte recognition. Although their initial use was primarily for disease detection and monitoring, there has been a recent resurgence in the detection of bio-warfare agents; and a great deal of U.S. federal funding has been directed to this purpose [36].

Most biosensors operate on the principle of molecular recognition. Antibodies, peptides, proteins, and DNA sequences all bind tightly to their target biomolecules with high specificity [37]. Dyes can be coupled to these recognition molecules to produce a fluorescent event when binding occurs. Quantum dot biosensors offer many benefits to those based on dye molecules. The surface of quantum dots can be easily altered, providing a facile route for conjugation to recognition molecules [38].

Additionally, their small size allows for incorporation into existing electronic devices. Several types of biosensors have been studied, but the most common utilize fluorescence resonance energy transfer (FRET) or the aggregation of fluorescent probes to detect analytes.

FRET-Based Biosensors

The simplest method for detection using fluorescent molecules is a system that produces an on or off signal upon binding. This can be accomplished using FRET. First, an electron in a fluorescent molecule is excited. Then, instead of decaying through photon emission, the energy in that electron is dissipated by transfer to a second molecule. This quenches the fluorescence of the first molecule. FRET is a distance dependent event. As the FRET donor and acceptor move away from each other, transfer no longer occurs and fluorescence in the donor is restored [39]. If a conformational change can be introduced upon analyte binding that separates the two molecules, a fluorescent on/off signal can be produced.

This has been accomplished in a number of systems. A combination of gold quantum dots (which do not fluoresce) and organic fluorophores have been utilized to create DNA sensors [40]. Gold quantum dots were bound

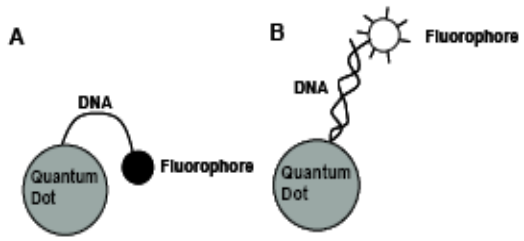

Figure 1.5: Detection of DNA binding through FRET. (A) Fluorophore-conjugated single stranded DNA is bound to a quantum dot, forming an arched structure with the nanoparticle surface. Fluorophore fluorescence is quenched through FRET with the nanoparticle. (B) When the complement DNA is added, the DNA structure changes, moving the fluorophore away from the nanoparticle and restoring fluorescence. Figure taken from [15].

to single stranded DNA sequences, which were terminated with fluorescent molecules, or fluorophores. The fluorophores formed an arched structure that interacted with the nanoparticle surface, quenching fluorescence (Figure 1.5). However, when the complement DNA was introduced, binding occurred and the conformation changed. The fluorophore migrated away from the quantum dot surface and its fluorescence was restored. This technique is very accurate, the mismatch of a single base pair in a 30 amino acid DNA sequence could be detected [40].

Several commercial companies have been setup in order to capitalise on the success of quantum dot labelling. These include Evident Technologies, Nanoprobes Inc., and Invitrogen Corporation which produce luminescent biomarkers, and NanoCarrier Co. Ltd and Nanomed Pharmceutical Inc. which provide nanoparticles for drug delivery.

Chapter 2

Ab-Initio Methods

2.1 Background

Quantum many-body methods and molecular dynamics simulations are increasingly used outside the orthodox fields of physics and chemistry. In particular, they are used increasingly in arguably the more challenging field of computational biology where the systems modeled are larger in physical size and, in general, are composed of more complex structures.

The ideal simulation of a biological process would include a quantum mechanical description of each electron and nucleon and the electrical forces between them. However, biological structures may be composed of just a few atoms to many thousands of atoms and therefore require efficient techniques in order to be modeled. Several quantum many-body techniques have been developed over the past decades and these involve a trade-off between accuracy and computational speed.

Quantum many-body methods are concerned with obtaining accurate properties of atoms, molecules, and larger complexes and structures from first principles (ab initio). The primary tool for doing this is the time-independent Schröodinger equation:

$$\widehat{H}\Psi = E\Psi, \tag{2.1}$$

where E is an energy eigenvalue, Ψ is the wavefunction and $\widehat{H}$ is the Hamiltonian given by

$$\widehat{H} = \sum_{i}^{N} -\frac{\hbar^2}{2m}\nabla_i^2 + \sum_{i}^{N} \frac{Qq}{|\mathbf{r}_i - \mathbf{R}|} + \sum_{i<j} \frac{q^2}{|\mathbf{r}_i - \mathbf{r}_j|}. \quad (2.2)$$

The Hamiltonian $\widehat{H}$ is the sum of three terms; from left to right, these are the kinetic energies of the electrons, the potential energy of each electron due to the nucleus, and the potential energies due to electronic interactions. Each of the nuclear coordinates is treated as a fixed parameter, and the quantum mechanical equations for the nuclei are solved separately (the Born-Oppenheimer approximation). [**sr: explain each term ?**]

[**sr: relevance to biosciences ?**]

2.2 Density Functional Theory

Overview of Theory

The main idea behind Density Functional Theory (DFT) is to formulate the quantum many-body problem in such a way that the wavefunction is a functional of the electron density which itself is the basic quantity of interest. The advantage in doing so is that the density is a function of three quantities (spatial coordinates) whereas the wavefunction is a function of $3N$ coordinates where N is the number of electrons. This approach is in contrast to many of the common methods for quantum many-body systems where the electronic wavefunction $\Psi(\mathbf{r}_i)$ is the basic quantity of interest.

Considering again the time-independent Schrödinger equation in the Born-Oppenheimer approximation, the electron density can be expressed in terms of the wavefunction as

$$n(\mathbf{r}) = N \int d^3\mathbf{r}_1 ... \int d^3\mathbf{r}_N \Psi^*(\mathbf{r}_i, ..., \mathbf{r}_N)\Psi(\mathbf{r}_i, ..., \mathbf{r}_N). \quad (2.3)$$

According to the Hohenberg-Kohn (HK) theorem, for ground states the above equation can be inverted; given a ground state electron density $n_0(\mathbf{r})$ it is possible, in principle, to calculate the corresponding ground-state wave function $\Psi_0(\mathbf{r}_i)$. This means that Ψ_0 is a functional of $n_0(\mathbf{r})$; $\Psi_0 = \Psi[n_0(\mathbf{r})]$. Consequently, all ground-state observables are functionals of $n_0(r)$ too. In

particular the energy can also be expressed as a functional of the charge density

$$E_0 = E[n_0] = \left\langle \Psi[n_0(\mathbf{r})] | \widehat{T} + \widehat{V} + \widehat{U} | \Psi[n_0(\mathbf{r})] \right\rangle . \tag{2.4}$$

DFT can be implemented in many ways. The minimization of an explicit energy functional, discussed up to this point, is not normally the most efficient among them. Much more widely used is the Kohn-Sham approach which involves the solution of the Schrödinger equation for non-interacting electrons

$$\left[-\frac{\hbar^2}{2m} \nabla_i^2 + V_s(\mathbf{r}) \right] \Phi_i(\mathbf{r}) = \epsilon_i \Phi_i(\mathbf{r}), \tag{2.5}$$

for orbitals $\Phi_i(\mathbf{r})$, where $V_s(\mathbf{r})$ potential of a single electron [**sr: verify this - why is it equivalent to the minimisation ? and comment on subscripts on r**], from which the charge density of the system is computed

$$n(\mathbf{r}) = \sum_i^N |\Phi_i|^2. \tag{2.6}$$

Since $V_s = V_s[n(\mathbf{r})]$, Equations (2.5) and (2.6) must be solved self consistently.

Applications

In physics applications, DFT is used to compute the ground state energy and wavefunctions of quantum systems. The theorems can be extended to the time-dependent domain (TDDFT), which can be also used to determine excited states. DFT has a vast number of applications in the biological sciences. These include fluorescence spectra of a protein [41], free energies of solvation of nucleic acid bases [42], and modeling of enzyme reactions [43] [44] [45]. Recently, DFT has been used to model quantum dots which have been used for biomedical imaging [].

2.3 Quantum Monte Carlo

Quantum Monte Carlo (QMC) refers to any method that utilises Monte Carlo techniques to perform quantum mechanical calculations. QMC is frequently applied in quantum many-body problems. As an example consider the evaluation of the energy of a wave function $\Psi(\mathbf{r_i})$ where $\mathbf{r}_i$ is a $3N$ dimensional position coordinate of N particles (for the remainder of this section, we drop the subscript from the $\mathbf{r}_i$ to avoid clutter),

$$E = \frac{\int d\mathbf{r}\Psi^*(\mathbf{r})\widehat{H}\Psi(\mathbf{r})}{\int d\mathbf{r}\Psi^*(\mathbf{r})\Psi(\mathbf{r})}, \tag{2.7}$$

where $\widehat{H}$ is the Hamiltonian operator. This is turned into an appropriate form for MonteCarlo integration by rewriting as

$$E = \int d\mathbf{r}\{\frac{|\Psi(\mathbf{r})|^2}{\int d\mathbf{r}|\Psi(\mathbf{r})|^2}\}[\Psi^*(\mathbf{r})\Psi(\mathbf{r})], \tag{2.8}$$

such that the quantity in braces has the form of a probability distribution. The integral is evaluated using Monte Carlo integration which may utilise the Metropolis algorithm for the choice of random numbers.

2.3.1 Variational Monte Carlo

Overview of Theory

Consider the following integral for the expectation value of the hamiltonian $\widehat{H}$ for a given trial wavefunction Ψ_T,

$$\left\langle \widehat{H} \right\rangle = \frac{\int d\mathbf{r}\Psi_T^*(\mathbf{r})\widehat{H}\Psi_T(\mathbf{r})}{\int d\mathbf{r}\Psi_T^*(\mathbf{r})\Psi_T(\mathbf{r})}. \tag{2.9}$$

Expansion of the wavefunction in the eigenstates of the hamiltonian through

$$\Psi_T(\mathbf{r}_i) = \sum_j a_j \Psi_j(\mathbf{r}_i), \tag{2.10}$$

results in

$$\left\langle \widehat{H} \right\rangle = \frac{\sum_{ij} a_i^* a_j \int d\mathbf{r} \Psi_i^*(\mathbf{r}) \widehat{H} \Psi_j(\mathbf{r})}{\sum_{ij} a_i^* a_j \int d\mathbf{r} \Psi_i^*(\mathbf{r}) \Psi_j(\mathbf{r})}, \tag{2.11}$$

which on evaluating the integrals results in

$$\frac{\sum_i a_i^2 E_i}{\sum a_i^* a_i} \geq E_0. \tag{2.12}$$

Thus the expectation value of the hamiltonian $\widehat{H}$ defined through equation (2.9) is an upper bound on the ground state energy E_0, of $\widehat{H}$. This is known as the variational principle and can be used to determine the ground state energy and wavefunction of a quantum many-body system. The procedure involves evaluating $\left\langle \widehat{H} \right\rangle$ for a trial wavefunction $\Psi_T(\mathbf{r}, \alpha)$ where $\mathbf{r}$ are the coordinate and α are variational parameters with respect to which $\langle H \rangle$ is minimised.

Applications

Ground state energies and wavefunction for atomic systems such as He, Be and Ne. Condensed matter applications such as Bose-Einstein condensation. [**sr: more applications in biosciences perhaps**]

2.3.2 Diffusion Monte Carlo

Overview of Theory

Consider the time dependent Schrödinger equation for a particle in some potential $V(\mathbf{r})$

$$i\frac{d\Psi(\mathbf{r}, t)}{dt} = \widehat{H}\Psi(\mathbf{r}, t). \tag{2.13}$$

Now, changing to imaginary time $\tau = it$ and adding a constant offset to the energy, we obtain

$$-\frac{d\Psi(\mathbf{r}, \tau)}{d\tau} = (\widehat{H} - E_0)\Psi(\mathbf{r}, \tau). \tag{2.14}$$

The state $\Psi(\mathbf{r}, \tau)$ can be expanded to a complete basis consisting of the stationary eigenstates of H and time-dependent coefficients $c(t)$,

$$\Psi(\mathbf{r},\tau) = c_0\Phi_0 + \sum_{i=1}^{\infty} c_i\Phi_i. \tag{2.15}$$

As a result of the linearity of the Schrödinger equation we can examine the evolution of each eigenfunction Φ_i separately. Considering Φ_0 first, we obtain $\frac{dc_0}{d\tau} = 0$ and therefore c_0 is a constant. Now considering any other Φ_i, we note $E_i > E_0$ and therefore from Schrödinger, $c_i \propto e^{-\tau}$. Thus we can determine E_0 by observing the amplitude of the wave function as we propagate through time; if it increases, then decrease the estimation of the offset energy or if the amplitude decreases, then increase the estimate of the offset energy.

The forward evolution of the wavefunction is achieved through a Green's function $G(\mathbf{r},\mathbf{r}',t)$,

[**sr: Perhaps compare with QMC**]

$$\Psi(\mathbf{r},\tau+d\tau) = \int G(\mathbf{r},\mathbf{r}',d\tau)\Psi(\mathbf{r},t)d\mathbf{r}'. \tag{2.16}$$

Applications
[**sr: Fill in some gaps here.**]

2.4 Hartree-Fock

The Hartree-Fock method assumes that the exact, N-body wavefunction of the system can be approximated by a single Slater determinant (in the case where the particles are fermions) or by a single permanent (in the case of bosons) of N spin-orbitals. It is the basis of molecular orbital (MO) theory, which posits that each electron's motion can be described by a single-particle function (orbital) which does not depend explicitly on the instantaneous motions of the other electrons. Therefore the Coulombic electron-electron repulsion is not "precisely" taken into account but only its average effect. Invoking the variational principle one can derive a set of N coupled equations for the N spin-orbitals. Solution of these equations yields the Hartree-Fock wavefunction and energy of the system, which are approximations of the exact ones.

Applications

[**sr: plenty in the biosciences**]

The electronic Schrdinger equation of atoms, molecules and solids but it has also found widespread use in nuclear physics. For molecules, Hartree-Fock is the central method for all ab initio quantum chemistry methods. Determination of the ground-state wavefunction and ground-state energy of a quantum many-body system. The computation of electronic structure of biological macromolecules in solution [46] and modelling enzyme reactions [47].

2.5 Other Approaches

2.5.1 Coupled Cluster

The Coupled Cluster (CC) method is a post Hartree-Fock molecular orbital method which adds a correction term to take into account electron correlation. It is perhaps the most reliable computational method of electronic structure theory for the prediction of molecular properties of well-behaved systems. However, the theoretical foundations involves technical details such as second quantisation, beyond the scope of this chapter. Hence the reader is directed to the literature.

Applications

CC is provides accurate electronic structure calculations for small to medium sized molecules. It is extensively used in nuclear physics. Other variants of the CC theory, such as equation-of-motion coupled cluster and multi-reference coupled cluster may also produce approximate solutions for the excited states of the system. [**sr: Certain that is has been used to analyse amino/nucleic acids**]. In biology, CC has been used to study nucleic acids [48].

2.5.2 Configuration Interaction

Configuration Interaction (CI) is a post Hartree-Fock linear variational method for solving the multi-electron Schrdinger equation within the Born-Oppenheimer approximation. A theoretical overview of CI is beyond the scope of this work and the reader is directed to the literature.

Applications

The long CPU time and immense hardware required for CI calculations means that the method is limited to relatively small systems. [**sr: perhaps some applications here.**] Modelling enzyme reactions [47].

2.5.3 Tight-Binding Model

In the tight binding model, it is assumed that the full Hamiltonian H of the system may be approximated by the Hamiltonian of an isolated atom centred at each lattice point. The atomic orbitals, which are eigenfunctions of the single atom Hamiltonian $\widehat{H}$, are assumed to be very small at distances exceeding the lattice constant. This is what is meant by tight-binding. A theoretical overview of CI is beyond the scope of this work and the reader is directed to the literature.

2.5.4 Semi-Empirical Quantum Chemistry Methods

Semi-empirical quantum chemistry methods are based on the Hartree-Fock formalism, but make many approximations and obtain some parameters from empirical data. They are very important in computational chemistry for treating large molecules where the full Hartree-Fock method without the approximations is too expensive. The use of empirical parameters appears to allow some inclusion of electron correlation effects into the methods.

Within the framework of Hartree-Fock calculations, some pieces of information (such as two-elecron integrals) are sometimes approximated or completely omitted. In order to correct for this loss, semi-empirical methods are parametrized, that is their results are fitted by a set of parameters, normally in such a way as to produce results that best agree with experimental data, but sometimes to agree with ab initio results.

Semi-empirical methods follow what are often called empirical methods where the two-electron part of the Hamiltonian is not explicitly included.

Semi-empirical calculations are much faster than their ab initio counterparts. Their results, however, can be very wrong if the molecule being computed is not similar enough to the molecules in the database used to parametrize the method.

Semi-empirical calculations have been most successful in the description of organic chemistry, where only a few elements are used extensively and molecules are of moderate size.

They have been used extensively in the modeling of enzyme reactions, for example, semi-empirical molecular orbital methods [49] [50] [51] [52]

Chapter 3

Molecular Dynamics

3.1 Background

Molecular dynamics (MD) is a numerical technique where atoms and molecules are allowed to interact for a period of time under known laws of physics. The laws may be classical or quantum mechanical or a combination of the two, giving a view of the motion of the atoms. Because molecular systems generally consist of a vast number of particles, it is impossible to find the properties of such complex systems analytically; MD simulation circumvents this problem by using numerical methods. It represents an interface between laboratory experiments and theory, and can be understood as a "virtual experiment".

Usually this is done by using one of the methods described for Ordinary Differential Equations (ODE's) to solve the coupled equations of motion for the atoms or molecules to be described. Molecular solids in particular can be studied by considering the molecules as rigid objects and using phenomenological classical equations of motion to describe the interaction between them.

A molecular dynamics simulation requires the definition of a potential function, or a description of the terms by which the particles in the simulation will interact. Potentials may be defined at many levels of physical accuracy; those most commonly used in chemistry are based on molecular mechanics and embody a classical treatment of particle-particle interactions that can reproduce structural and conformational changes but usually cannot reproduce chemical reactions. When finer levels of detail are required, potentials based on quantum mechanics are used; some techniques attempt to create hybrid classical/quantum potentials where the bulk of the system is

treated classically but a small region is treated as a quantum system, usually undergoing a chemical transformation.

As a simple example the LennardJones potential given by

$$\Phi(r) = \epsilon((\frac{a}{r})^{0.5} - 2(\frac{a}{r})^{6}), \tag{3.1}$$

has been successfully used to describe the thermodynamics of noble gases.

Consider a set of particles interacting through a twobody potential, $\Phi(r)$. The equations of motion can be written in the form

$$\frac{dr_i}{dt} = v_i, \tag{3.2}$$

$$\frac{dv_i}{dt} = -\frac{1}{m}\frac{\partial}{\partial r_i}\sum_{j\neq i}\Phi(|r_i - r_j|). \tag{3.3}$$

Such a problem can be solved through standard techniques for ODE's such as the Leapfrog method.

[**sr: perhaps re-word slightly**] Ab-initio quantum-mechanical formulae may be used to calculate the potential energy of a system of atoms or molecules. Compared to a classical potential function, which is represented by empirical functions, the properties of the system in ab-intio calculations are the wave-functions for electrons moving around the nucleus of atoms. This calculation is usually made "locally", i.e., for nuclei in the close neighborhood of the reaction coordinate. Although various approximations may be used, these are based on theoretical considerations, not on empirical fitting. Ab-Initio produce a large amount of information that is not available from the empirical methods, such as density of states information. Of course, the computational price paid is high. A significant advantage of using ab-initio methods is the ability to study reactions that involve breakage or formation of covalent bonds, and this would correspond to multiple electronic states. Classical molecular dynamics is unable to simulate breakage and formation of covalent bonds, However, in recent years techniques such as thermodynamic integration and ghost particles have been introduced to overcome these limitations. The success however remains limited.

3.2 Example Applications

In physics, MD is used to examine the dynamics thin film growth and ion-subplantation. It is also used to examine the physical properties of nanotechnological devices that are being developed.

In chemistry, MD serves as an important tool in protein structure determination and refinement using experimental tools such as X-ray crystallography and NMR.

In biology, the first macromolecular MD simulation, published (1977, Size: 500 atoms, Simulation Time: 0.0092 ns. Protein: Bovine Pancreatic Trypsine Inhibitor. This is one of the best studied proteins in terms of folding and kinetics.

The simulation of the complete satellite tobacco mosaic virus (STMV) (2006, Size: 1 million atoms, Simulation time: 50 ns).

Chapter 4

Computational Modeling of Nanocrystals

Although substantial experimental progress has been made in the application of semiconductor nanocrystals to biological applications, the results have been achieved only through experimental trial-and-error optimisation of the physical and chemical properties, as crystal growth mechanisms and nanocrystal-ligand interaction, are not fully understood.

Experimental progress in the use of nanoscale systems for biomedical applications could be accelerated through accurate theoretical models which have the ability to predict the optical and electronic properties of functionalized nanoclusters and therefore design the optimal nanoclusters for specific biomedical applications. The nanocrystals consist of between 10 and 100000 atoms and exhibit quantum mechanical effects. Therefore, one requires the use of quantum many-body techniques for an accurate description.

4.1 Application of Ab-Intio Methods

Currently, there is much theoretical research on the effects of nanocrystal size on the optical and electronic properties of semiconductor nanocrystals. As discussed in Chapter **??**, the size of the nanocrystal beyond some threshold value has dramatic effects on its properties, due to the increasing importance of surface effects. The objectives of researchers in the field are to explain the observed dependance of the optical and electronic properties on cluster size for the full range of sizes for which size effects are observed.

An accurate description will include surface effects (crystal defects, dangling bonds etc.) and treat individual atoms including those of the organic ligands (in functionalised clusters for biological applucations) essential for biological applications. Optical properties of the clusters have been shown to depend strongly on the ligand sructure [53, 54, 55].

Early theoretical models [14] to describe quantum size effects on CdS nanocrystals were based on the effective mass approximation for lattice-like effects and a particle in a box model to include quantum confinement. The models demonstrated an increase in the lowest energy transition as cluster size is decreased within a suitable range. However, the descriptions were consistent with experimental data only for large clusters, as the models failed to include a realistic description of surface effects.

Consistancy with experimental observations for smaller clusters was achieved in subsequent work which made improvements on the effective mass approximation by including the use of empirical pseudo potentials (see Section **??**), by Krishna *et al.* [56] or the use of tight-binding theory, by Lippens *et al.* [57] and Hill *et al.* [58]. Only the work by Hill *et al.* included surface effects although they did not take into account the presence of ligand atoms which would be essenial for biomedical applications.

Ab initio methods were employed by Liu *et al.* [59] to model ligand capped clusters of CdS. They used a semiempirical method (see **??**) to obtain good agreement between experimental and theoretcial data. The configuration interaction with single excitations (CIS) scheme was employed to improve the description of excited states. Due to computationally intensive nature of the technique, only small clusters were modeled. The clusters included $[Cd(SPh)_4]^{2-}$ which were typically much smaller than those utilized in biomedical applications.

In condensed matter physics, density functional theory (DFT) is frequently used to model systems with 100s of atoms and therefore in principle one could expect it to be applied to some of the quantum dots of the size relevent to biomedical applications.

During recent years, research involving the application of ab-inito techniques, in particular DFT and Quantum Monte Carlo (QMC), into modelling semiconductor nanoclusters has grown steadily.

Typically, ab-initio molecular dynamics (MD) techniques are used to predict the structural and electronic properties of semiconductor dots interfaced with desired organic media and QMC were employed to compute optical gaps whilst accurately treat ing the effects of exchange and correlation.

The physical and chemical properties of a range of nanoclusters of varying material, size and ligand binding have been explored. Some of the earlier work concerned the effect of surface passivants on the optical gaps of Si nanoclusters [60]. Using both DFT and QMC techniques it was shown that significant changes occur in the gap of fully hydrogenated nanoclusters when the surface contains passivants other than hydrogen, in particular atomic oxygen. The reduction in the optical gap as a function of nanocluster size were computed for sizes below 2ñm with the results being consistent with experimental observations. In subsequent work, the accuracy of DFT and EMP calculations were examined by comparison with QMC [61].

The QMC method has also been employed to study of the surface formation energies of clusters larger than a few atoms. A set of atomic surface and step reconstructions, present only on highly curved nanoparticles were examined. The thermodynamic stability of these nanosurfaces was predicted under different synthesis conditions and the effects of these surface reconstructions on the optoelectronic properties are also examined [62].

Initial applications of DFT to CdSe nanocrystals involved using time-dependent DFT to compute the absorption spectra and optical gaps [63]. The investigations were performed on Cd_nSe_n ($n = 17, 26, 38$). The results appeared to be in good agreement with experimental data.

Structural properties of CdSe nanocrystals with diameters ranging upto 1.5 nm and in the presence of organic ligands were investigated in subsequent work [64]. The predicted CdSe atomic structures were found to be insensitive to the presence of surface passivation when compared to Si, Ge and III-V nanoclusters.

More recently, DFT has been utilized to investigate the influence of organic ligands on crystal growth on different facets of a wurtzite CdSe crystal [65]. The investigations included preferred binding sites and geometries, vibrational frequencies and binding energetics of phospine, carboxylic acid, and phosphinic acid model ligands.

4.2 Quantum Dot Intermittancy

An interesting phenomenon observed with single semiconductor nanocrystals is the turning on and off of the florescence as the crystal is subject to continuous excitation. The fluorescence intermittancy or “blinking” has been observed in individual nanocrystals of CdSe to have a characterisitc time

timescale of 0.5 s and is generally not observed in large ensembles [66].

The fluorescence intermittancy reduces the quantum yield of the dots and could potentially limit the use of nanocrytals for some biological applications. Hence it is important to understand the phenomenon and find techniques to overcome it.

The origin of fluorescence intermittency has been studied in detail [67, 68, 69]. It is now generally accepted that the effect arises from rare ionization events that eject a carrier from the quantum dot [67, 68]. An Auger ionization model has been proposed by Efros *et al.* [69] to explain the quantum dot fluorescence intermittency. The relaxation of a bi-excition following the Auger process was assumed to lead to ionization of the quantum dot, which consequently became non-fluorescent.

Although fluorescence intermittency has long been considered as an intrinsic property of CdSe quantum dots, very recent results [70] demonstrated that the intermittency of single QDs could be significantly reduced by chemical processes. Surrounding the quantum dots with a concentrated solution of molecules containing thiol groups (such as betamercaptoethanol or DTT) suppresses the blinking.

An interesting theoretical work by Wang [71] investigated the influence of external charges on the radiative recombination rate of an electron-hole pair in a CdSe quantum dot through an empirical pseudopotential calculation. Wang showed that the presence of an electron on the surface of a CdSe quantum dot could through Coulomb forces reduce the locality of the charges in the bound exciton. A reduction in the overlap of the excitonic electron and hole wavefunctions resulted in reduction in the recombination rate by a factor of 70.

Appendix

.1 Resources

- **DFT software, CASTEP** http://www.tcm.phy.cam.ac.uk/castep/
- **DFT software, DFT++** http://dft.physics.cornell.edu/

.2 Research and Commercial Organisations

- *** Winter Group, Univ. of Texas, Austin : Experimental bionanoscience** http://www.chbmeng.ohio-state.edu/~winter/links/index.html
- *** Alivisatos Group, Berkely : Experimental bionanoscience** http://www.cchem.berkeley.edu/pagrp/overview.html
- **Weiss Group, UCLA** http://www.chem.ucla.edu/dept/Faculty/sweiss/
- *** Bawendi Group, MIT** http://nanocluster.lms.mit.edu/
- **Gao Lab, Washington** http://faculty.washington.edu/xgao/index.html
- *** Lawrence Livermore Lab., Quantum Simulations Group : Computational modelling of biological nanotags** http://physci.llnl.gov/Research/qsg-old/
- **Madura Group, Duquesne : Computational modelling of nanocrystals** http://vidar.chemistry.duq.edu/faculty/madura/index.html
- **Zhou : Computational modelling of nanocrystals** http://bilbo.bio.purdue.edu/~zhou/

- **Quantum Dots/Semiconductor Nanocrystals** http://www.evidenttech.com/qdot-definition/quantum-dot-about.php

Bibliography

[1] C. Mah, I. Zolotukhin, T. J. Fraites, J. Dobson, C. Batich, and B. J. Byrne. Microsphere- mediated delivery of recombinant aav vectors in vitro and in vivo. *Mol. Therapy*, 1, 2000.

[2] D. Panatarotto, C. D. Prtidos, J. Hoebeke, F. Brown, E. Kramer, J. P. Briand, S. Muller, M. Prato, and A. Bianco. Immunization with peptide-functionalized carbon nanotubes enhances virus-specific neutralizing antibody responses. *Chemistry & Biology*, 10:961–966, 2003.

[3] R. L. Edelstein, C. R. Tamanaha, P. E. Sheehan, M. M. Miller, D. R. Baselt, L. J. Whitman, and R. J. Colton. The barc biosensor applied to the detection of biological warfare agents. *Biosensors Bioelectron.*, 14:805–813, 2000.

[4] J. M. Nam, C. C. Thaxton, and C. A. Mirkin. Nanoparticles-based bio-bar codes for the ultrasensitive detection of proteins. *Science*, 301:1884–1886, 2003.

[5] R. Mahtab, J. P. Rogers, and C. J. Murphy. Protein-sized quantum dot luminescence can distinguish between "straight", "bent", and "kinked" oligonucleotides. *J. Am. Chem. Soc.*, 117:9099–9100, 1995.

[6] J. Ma, H. Wong, L. B. Kong, and K. W. Peng. Biomimetic processing of nanocrystallite bioactive apatite coating on titanium. nanotechnology. *J. Am. Chem. Soc.*, 14:619–623, 2003.

[7] A. de la Isla, W. Brostow, B. Bujard, M. Estevez, J. R. Rodriguez, S. Vargas, and V. M. Castano. Nanohybrid scratch resistant coating for teeth and bone viscoelasticity manifested in tribology. *Mat. Resr. Innovat.*, 7:110–114., 2003.

[8] M. Bruchez, M. Moronne, P. Gin, S. Weiss, and A. P. Alivisatos. Semiconductor nanocrystals as fluorescent biological labels. *Science*, 281:2013–2016, 1998.

[9] W. C. W. Chan and S. M. Nie. Quantum dot bioconjugates for ultrasensitive nonisotopic detection. *Science*, 281:2016–2018., 1998.

[10] S. Wang, N. Mamedova, N. A. Kotov, W. Chen, and J. Studer. Antigen/antibody immunocomplex from cdte nanoparticle bioconjugates. *Nano Letters*, 2:817–822, 2002.

[11] L. E. Brus. *Appl. Phys. A*, 53:456, 1991.

[12] A. N. Goldstein, C. M. Echer, and A. P. Alivisatos. *Science*, 256:1425, 1992.

[13] K. Kalyanasundaram, E. Borgarello, D. Duonghong, and M. Grtzel. Cleavage of water by visible-light irradiation of colloidal cds solutions: Inhibition of photocorrosion by ruo2. *Angew. Chem. Int. Ed. Engl*, 20(11):987–988, 1981.

[14] H. Weller, H. M. Schmidt, U. Koch, A. Fojtik, S. Baral, A. Henglein, W. Kunath, K. Weiss, and E. Dieman. Photochemistry of colloidal semiconductors. onset of light absorption as a function of size of extremely small cds particles. *Chem. Phys. Lett.*, 124(6):557, 1986.

[15] Winter. Development and optimization of quantum dotneuron interfaces. *PhD Thesis, University of Texas at Austin*, 2004.

[16] X. Michalet, F. F. Pinaud, L. A. Bentolila, J. M. Tsay, S. Doose, J. J. Li, G. Sundaresan, A. M. Wu, S. S. Gambhir, and S. Weiss. Quantum dots for live cells, in vivo imaging, and diagnostics. *Science*, 307:538–544, 2005.

[17] F. Pinaud, D. King, H.-P. Moore, and S. Weiss. *J. Am. Chem. Soc.*, 126:6115, 2004.

[18] W. Guo, J. J. Li, Y. A. Wang, and X. G. Peng. *Chem. Mater.*, 15:3125, 2003.

[19] J. Gao and D. G. Truhlar. Quantum mechanical methods for enzyme kinetics. *Annual Review of Physical Chemistry*, 53:467–505, 2002.

[20] B. Dubertret, P. Skourides, D. J. Norris, V. Noireaux, A. H. Brivanlou, and A. Libchaber. In vivo imaging of quantum dots encapsulated in phospholipid micelles. *Science*, 298:1759, 2002.

[21] G. P. Mitchell, C. A. Mirkin, and R. L. Letsinger. *J. Am. Chem. Soc.*, 121:8122, 1999.

[22] M. A. Hines and P. Guyot-Sionnest. Synthesis and characterization of strongly luminescing zns-capped cdse nanocrystals. *J. Phys. Chem. 100*, 468.

[23] M. Dahan, S. Lvi, C. Luccardini, P. Rostaing, B. Riveau, and A. Triller. Diffusion dynamics of glycine receptors revealed by single-quantum dot tracking. *Science*, 302:442, 2003.

[24] W. J. Parak, R. Boudreau, M. Le Gros, D. Gerion, D. Zanchet, C. M. Micheel, S. C. Williams, A. P. Alivisatos, and C. Larabell. Cell motility and metastatic potential studies based on quantum dot imaging of phagokinetic tracks. *Adv. Mats.*, 14(12):882, 2002.

[25] L. C. Mattheakis, J. M. Dias, Y.-J. Choi, J. Gong, M. P. Bruchez, J. Liu, and E. Wang. Optical coding of mammalian cells using semiconductor quantum dots. *Anal. Chem.*, 327, 2004.

[26] X. Gao, Y. Cui, R. M. Levenson, L. W. K. Chung, and S. Nie. *Nature Biotech.*, 22, 2004.

[27] S. Stolik, J. A. Delgado, A. Perez, and L. Anasagasti. Measurement of penetration depths of red and near infrared light in human "ex vivo" tissues. *J. Photochem. Photobiol.*, B 57:90, 2000.

[28] J. B. Lansman, P. Hess, and R. W. Tsien. Blockade of current through single calcium channels by cd^{2+}, mg^{2+}, and ca^{2+}. *J. Gen. Physio l.*, 88:321, 1986.

[29] M. P. Waalkes. Cadmium carcinogenesis. *Mut. Res.*, 533:107, 2003.

[30] A. M. Derfus, W. C. W. Chan, and S. N. Bhatia. Probing the cytotoxicity of semiconductor quantum dots. *Nano Lett.*, 4(1):11, 2004.

[31] D. R. Larson, W. R. Zipfel, R. M. Williams, S. W. Clark, M. P. Bruchez, F. W. Wise, and W. W. Webb. Water-soluble quantum dots for multiphoton fluorescence imaging in vivo. *Science*, 300:1434, 2003.

[32] W. C. W. Chan, D. J. Maxwell, X. Gao, R. E. Bailey, M. Han, and S. Nie. Luminescent quantum dots for multiplexed biological detection and imaging. *Curr. Opin. Biotech.*, 13:40, 2002.

[33] M. E. Akerman, W. C. W. Chan, P. Laakkonen, S. N. Bhatia, and E. Ruoslahti. Nanocrystal targeting in vivo. *Proc. Nat. Acad. Sci.*, 99(20):12617, 2002.

[34] C. Seydel. Quantum dots get wet. *Science*, 300:80, 2003.

[35] X. Wu, H. Liu, J. Liu, K. N. Haley, J. A. Treadway, J. P. Larson, N. Ge, F. Peale, and M.P. Bruchez. Immunofluorescent labeling of cancer marker her2 and other cellular targets with semiconductor quantum dots. *Nature Biotech.*, 21:41, 2003.

[36] S. Bunk. Sensing evil. *The Scientist*, 16(15):13, 2002.

[37] J. A. McCammon. Theory of biomolecular recognition. *Curr. Opin. Struct. Biol.*, 8(2):245, 1998.

[38] A. P. Alivisatos. Perspectives on the physical chemistry of semiconductor nanocrystals. *J. Phys. Chem.*, 100:13226, 1996.

[39] L. Stryer and R. P. Haugland. Energy transfer: A spectroscopic ruler. *Proc. Natl. Acad. Sci.*, 58(2):719, 1967.

[40] D. J. Maxwell, J. R. Taylor, and S. Nie. Self-assembled nanoparticle probes for recognition and detection of biomolecules. *J. Am. Chem. Soc.*, 124:9606, 2002.

[41] M. A. L. Marques, X. Lopez, D. Varsano, A. Castro, and A. Rubio. Time-dependent density-functional approach for biological chromophores: The case of the green fluorescent protein. *Phys. Rev. Lett.*, 90:258101, 2003.

[42] J. Li, C. J. Cramer, and D. G. Truhlar. Application of a universal solvation model to nucleic acid bases: comparison of semiempirical molecular

orbital theory, ab initio hartree-fock theory, and density functional theory. *Biophys. Chem.*, 78:147–55, 1999.

[43] A. D. Becke. *Phys. Rev. A*, 38:3098, 1988.

[44] C. T. Lee, W. T. Yang, and R. G. Parr. *Phys. Rev. B*, 37:78589, 1988.

[45] P. J. Stephens, F. J. Devlin, C. F. Chabalowski, and M. J. Frisk. *J. Phys. Chem.*, 98:11623–27, 1998.

[46] D. M. York, T.-S. Lee, and W. Yang. Quantum mechanical treatment of biological macromolecules in solution using linear-scaling electronic structure methods. *Phys. Rev. Lett.*, 80, 1998.

[47] W. J. Hehre, L. Radom, P. V. R. Schleyer, and J. A. Pople. *Ab Initio Molecular Orbital Theory.* New York: Wiley, 1986.

[48] O. Bludsk, J. Poner, and J. Leszczynski. Amino groups in nucleic acid bases, aniline, aminopyridines, and aminotriazine are nonplanar: Results of correlated ab initio quantum chemical calculations and anharmonic analysis of the aniline inversion motion. *J. Chem. Phys.*, 105:11042–11050, 1996.

[49] J. A. Pople, D. P. Santry, and G. A. Segal. *J. Chem. Phys.*, 43:129135, 1965.

[50] M. J. S. Dewar, E. G. Zoebisch, E. F. Healy, and J. J. P. Stewart. *J. Am. Chem. Soc.*, 107:39023909, 1985.

[51] J. J. P. Stewart. *J. Comput. Aided Mol. Des.*, 4:1105, 1990.

[52] M. J. S Dewar and W. Thiel. *J. Am. Chem. Soc.*, 99:48994907, 1990.

[53] N. Herron, J. C. Calabrese, W. E. Farneth, and Y. Wang. Crystal structure and optical properties of $cd_{32}s_{14}(sc_6h_5)_{36}{\cdot}dmf_4$, a cluster with a 15 angstrom cadmium sulfide core. *Science*, 259:14261428, 1993.

[54] T. Vossmeyer, G. Reck, L. Katsikas, E. T. K. Haupt, B. Schulz, and H. Weller. A double-diamond superlattice built up of $cd_{17}s_4(sch_2ch_2oh)_{26}$ clusters. *Science*, 267:14761479, 1995.

[55] T. Vossmeyer, G. Reek, B. Schulz, L. Katsikas, and H. Weller. Double-layer superlattice structure built up of $cd_{32}s_{14}(sch_2ch(oh)ch_3)_{36}$*- $4h_2o$ clusters. *J. Am. Chem. Soc.*, 117:1288112882, 1995.

[56] R. Krishna and R. A. Friesner. Quantum confinement effects in semiconductor clusters. *J. Phys. Chem.*, 95(11):83098322, 1991.

[57] P. E. Lippens and M. Lannoo. Comparison between calculated and experimental values of the lowest excited electronic state of small cdse crystallites. *Phys. Rev. B*, 41:6079, 1990.

[58] N. A. Hill and K. B. Whaley. Electronic structure of semiconductor nanoclusters: A time-dependent theoretical approach. *J. Chem. Phys.*, 99(5):37073715, 1993.

[59] H. Liu, J. T. Hupp, and M. A. Ratner. Electronic structure and spectroscopy of cadmium thiolate clusters. *J. Chem. Phys.*, 100:1220312213, 1996.

[60] A. Puzder, A. J. Williamson, J. Grossman, and G. Galli. Surface chemistry of silicon nanoclusters. *Phys. Rev. Lett.*, 88, 2002.

[61] A. J.Williamson, J. C. Grossman, R. Q. Hood, A. Puzder, and G. Galli. Quantum monte carlo calculations of nanostructure optical gaps: Application to silicon quantum dots. *Phys. Rev. Lett.*, 89, 2002.

[62] A. Puzder, A. J. Williamson, F. A. Reboredo, and G. Galli. Structural stability and optical properties of nanomaterials with reconstructed surfaces. *Phys. Rev. Lett.*, 91, 2003.

[63] M. C. Troparevsky, L. Kronik, and J. R. Chelikowsky. Optical properties of cdse quantum dots. *J. Chem. Phys.*, 119(4):22842287, 2003.

[64] A. Puzder, A. J. Williamson, F. Gygi, and G. Galli. Self-healing of cdse nanocrystals: First-principles calculations. *Phys. Rev. Lett.*, 92, 2004.

[65] J. Y. Rempel, B. L. Trout, M. G. Bawendi, and K. F. Jensen. Density functional theory study of ligand binding on cdse (0001), (0001h), and (112h0) single crystal relaxed and reconstructed surfaces: Implications for nanocrystalline growth. *J. Phys. Chem. B*, 110:18007–18016, 2006.

[66] M. Nirmal, B. O. Dabbousi, M. G. Bawendi, J. J. Macklin, J. K. Trautman, T. D. Harris, and L. E. Brus. Fluorescence intermittency in single cadmium selenide nanocrystals. *Nature*, 383:802–804, 1996.

[67] M. Kuno, D. P. Fromm, H. F. Hamann, A. Gallagher, and D. J. Nesbitt. *J. Chem. Phys.*, 115:1028, 2001.

[68] M. Kuno, D. P. Fromm, S. T. Johnson, A. Gallagher, and D. J. Nesbitt. *Phys. Rev. B*, 67:125304, 2003.

[69] A. L. Efros and M. Rosen. *Phys. Rev. Lett.*, 78:1110, 1997.

[70] S. Hohng and T. Ha. *J. Am. Chem. Soc.*, 126:1324, 2004.

[71] Lin-Wang Wang. Calculating the influence of external charges on the photoluminescence of a cdse quantum dot. *J. Phys. Chem. B*, 105:2360–2364, 2001.